Neuroinform (2013) 11:159–173
DOI 10.1007/s12021-012-9161-2

ORIGINAL ARTICLE

A Systems-Level Approach to Human Epileptic Seizures

Christian Rummel · Marc Goodfellow · Heidemarie Gast · Martinus Hauf · Frédérique Amor · Alexander Stibal · Luigi Mariani · Roland Wiest · Kaspar Schindler

Published online: 8 September 2012

Abstract Epileptic seizures are due to the pathological collective activity of large cellular assemblies. A better understanding of this collective activity is integral to the development of novel diagnostic and therapeutic procedures. In contrast to reductionist analyses, which focus solely on small-scale characteristics of ictogenesis, here we follow a systems-level approach, which combines both small-scale and larger-scale analyses. Peri-ictal dynamics of epileptic networks are assessed by studying correlation within and between different spatial scales of intracranial electroencephalographic recordings (iEEG) of a heterogeneous group of patients suffering from pharmaco-resistant epilepsy. Epileptiform activity as recorded by a single iEEG electrode is determined objectively by the signal derivative and then subjected to a multivariate analysis of correlation between all iEEG channels. We find that during seizure, synchrony increases on the smallest and largest spatial scales probed by iEEG. In addition, a dynamic reorganization of spatial correlation is observed on intermediate scales, which persists after seizure termination. It is proposed that this reorganization may indicate a balancing mechanism that decreases high local correlation. Our findings are consistent with the hypothesis that during epileptic seizures hypercorrelated and therefore functionally segregated brain areas are re-integrated into more collective brain dynamics. In addition, except for a special sub-group, a highly significant association is found between the location of ictal iEEG activity and the location of areas of relative decrease of localised EEG correlation. The latter could serve as a clinically important quantitative marker of the seizure onset zone (SOZ).

Keywords Epileptic focal onset seizures · Quantitative EEG · High frequency oscillations · Pre-surgical evaluation · Seizure onset zone

Abbreviations
CC equal-time cross-correlation

Electronic supplementary material The online version of this article (doi:10.1007/s12021-012-9161-2) contains supplementary material, which is available to authorized users.

C. Rummel (✉) · M. Hauf · R. Wiest
Support Center for Advanced Neuroimaging (SCAN), University Institute of Diagnostic and Interventional Neuroradiology, Inselspital, Bern University Hospital, University of Bern, 3010 Bern, Switzerland
e-mail: crummel@web.de

M. Goodfellow
Systems Biology Doctoral Training Centre, Manchester Institute of Biotechnology, The University of Manchester, Manchester, UK

M. Goodfellow
Centre for Interdisciplinary Computational and Dynamical Analysis (CICADA), School of Mathematics, The University of Manchester, Manchester, UK

H. Gast · F. Amor · K. Schindler
qEEG group, Department of Neurology, Inselspital, Bern University Hospital and University of Bern, Bern, Switzerland

A. Stibal
Department of Neurosurgery, Inselspital, Bern University Hospital, University of Bern, Bern, Switzerland

L. Mariani
Department of Neurosurgery, Basel University Hospital, University of Basel, Basel, Switzerland

EEG	electroencephalogram
FLE	frontal lobe epilepsy
Fo	foramen ovale
iEEG	intracranial electroencephalogram
MRI	magnetic resonance imaging
PLE	parietal lobe epilepsy
TCS	total correlation strength
TLE	temporal lobe epilepsy
SCC	slope cross-correlation
SOZ	seizure onset zone

Introduction

Epilepsy is one of the most prevalent neurological disorders, with the number of patients estimated to be at least 50 million worldwide (de Boer et al. 2008). Epileptic seizures are not only detrimental to patients' health and even life threatening (Lin and Benbadis 2009), but they also place a heavy psychosocial and economic burden on patients' families (Smith et al. 2009) and on society at large (Zachry et al. 2009). In addition, one out of four patients undergoing currently available treatment will continue to suffer from epileptic seizures (Elger and Schmidt 2008; Lüders 2008).

Therefore it is of paramount importance to develop more efficient therapies for epilepsy, including new anti-seizure drugs and diagnostic tools. The latter will enable a greater degree of individualization in the surgical resection of epileptogenic brain areas. To facilitate these developments, it has been proposed that seizure mechanisms should be elucidated not only on the purely reductionist (sub-) cellular level, but complementarily on the systems-level (Spencer 2002; Schindler et al. 2007b; Blumenfeld et al. 2009). Otherwise stated, the aim is not to focus solely on the parts, but also on the whole and on the relation between the parts and the whole.

The rationale for this approach is at least threefold. First, a systems perspective takes into account that epileptic seizures are produced by the collective electrical activity of spatially distributed and interacting neuronal networks (Bartolomei et al. 2001; McCormick and Contreras 2001; Blumenfeld et al. 2004; Schiff et al. 2005; Guye et al. 2006; Weder et al. 2006). Second, from a practical point of view, the electrical activity and interactions of these cellular assemblies may be assessed by electroencephalography (EEG) and may thus provide patient-specific and diagnostically highly relevant information (Rosenow and Lüders 2001). Third, invoking EEG recordings allows one to assess local and global neuronal correlation (Schindler et al. 2010) and thus places the problem of understanding the network mechanisms of seizures within the broader context of coordination between spatially distributed activity in the central nervous system. Specifically, it has been proposed that physiological brain activity relies on a balance between local and global synchrony (Silberstein 1995; Varela et al. 2001). This balanced state is considered to be optimal for the self-organised, cross-scale coordination of neuronal assemblies (Tononi et al. 1994; Friston et al. 1995; Bressler and Kelso 2001; Stam and Reijneveld 2007). As a corollary, deviations towards excessive local or global synchrony are regarded as potential characteristics of diverse neurological or psychiatric diseases (Uhlhaas and Singer 2006).

Epileptic seizures are classically understood as globally synchronised brain states, an interpretation that has recently been challenged, see e.g. Wendling et al. (2003); Schiff et al. (2005); Schindler et al. (2007a, b), Kramer et al. (2010) or Frei et al. (2010). On the other hand it has been shown that epileptogenic cortex might be characterised by increased local EEG synchrony and/or correlation (Schevon et al. 2007; Dauwels et al. 2009; Schindler et al. 2010). The present study proceeds from the idea that at the systems level these patches of local hypersynchrony constitute an abnormally segregated dynamic state. Combining uni-, bi- and multivariate EEG analysis methods, we here investigate the hypothesis that during epileptic seizures these functionally segregated brain areas are re-integrated into more collective dynamics.

As pointed out recently by Zaveri in the debate regarding current controversial topics in epilepsy (Frei et al. 2010) "measurements are typically performed at a single scale and ignore the possibility that synchrony can be different at different scales". Using the systems perspective we address the peri-ictal spatial reorganization of neuronal synchrony on different spatial scales in a quantitative manner. Besides the general context of improving our understanding of the pathophysiology of epileptic seizures, the systems perspective can potentially help to separate the seizure onset zone (SOZ) from the seizure propagation zone. The objective delineation of the SOZ is of high clinical relevance because it is currently considered to be the best approximation of the epileptogenic zone, which has been defined as the brain area that has to be surgically removed in order to render a patient suffering from pharmacoresistent epilepsy seizure free (Rosenow and Lüders 2001; David et al. 2011).

Materials and Methods

Patients

The data set consisted of 60 peri-ictal iEEG seizure recordings from eight patients suffering from longstanding pharmacoresistant epilepsy with focal-onset seizures. All patients were potential candidates for epilepsy surgery. In this heterogeneous patient group non-invasive studies had not provided an unequivocal localisation of SOZs and

therefore the patients underwent long-term iEEG recordings at the Inselspital Bern in 2008 and 2009. The decision to implant electrodes as well as decisions regarding the electrode targets and the duration of implantation were made entirely on clinical grounds without reference to the present retrospective research study, which was approved by the ethics committee of the Kanton of Bern. All the patients gave written informed consent that the data from their long-term EEG might be used for research purposes. Clinical information regarding the patients is summarised in Tables 1 and 2. During long term EEG, patients had two to nineteen focal-onset seizures lasting from 33 to 429 s. Epilepsy surgery was performed in five patients, who subsequently became seizure free for at least 1 year. After the period given in Table 2, patients either reverted to having seizures or else their case was closed.

EEG Data

Patients were implanted with foramen ovale, strip, grid and depth electrodes with 40 to 104 contacts in total (see Table 3). The iEEG was recorded using a NicoletOne™ recording system. For a detailed description of the amplifier specifications see Schindler et al. (2010).

The sampling rate was 1,024 Hz for recordings with up to 64 iEEG channels and 512 Hz otherwise. In all cases, the iEEG was referenced to an extracranial electrode for the original recording and re-referenced to the common median of all artifact-free signals (the number of which is denoted as M in the following) before analysis. Artifact-free channels were visually selected by an experienced epileptologist/electroencephalographer (K.S.). Signals were filtered in the range of 0.5 to 150 Hz using third order Butterworth filters.

The analysed iEEG segments were 15 to 30 min in duration and contained at least 5 min of pre-ictal and 4 min post-ictal recording. Seizure activity, as well as seizure onset and termination times, were visually defined by an experienced epileptologist/electroencephalographer (K.S.).

Data Analysis

Our systems-level analysis of iEEG data consisted of a suite of complementary, quantitative measures operating at three different spatial scales. In terms of the dimensions of the iEEG electrodes used, these three scales represent i) the collective activity of a large number of neurons beneath a single contact, ii) the collective activity of all contacts on all electrodes and iii) the contribution of single contacts to the whole.

Univariate signals provide information regarding (i), whereas bivariate and multivariate measures of interrelation are used to investigate (ii) and (iii). More specifically, quantitative analyses of the eigenvalues and eigenvectors of interrelation matrices address scales (ii) and (iii), respectively. Each of these methods is described in detail in the following three sections.

Univariate Analysis: Objective Detection of Epileptiform Activity

After defining seizure occurrence by visual inspection of the iEEG, the absolute signal slopes (more precisely an approximation to the first temporal derivative of the signals) were used to detect epileptiform activity in single EEG channels in an independent and objective way, as previously described in Schindler et al. (2007b). The effect of temporal differentiation on EEG signals is investigated in more detail in (Takigawa et al. 1994; Majumdar and Vardhan 2011). In

Table 1 Patient and seizure characteristics

ID	Sex	Age [y]	Epilepsy duration [y]	Seizure type	iEEG seizure onset	MRI outcome	No. of seizures	Seizure duration [s]
1	M	18	14	TLE	temporo-polar, mesio-temporal right	right hippocampal and hemispheric atrophy	5	192±49
2	M	26	18	TLE	temporal left and right	normal	5	150±62
3	M	27	20	TLE	temporo-lateral, mesio-temporal left	normal	9	146±32
4	F	49	43	FLE	gyrus front. med. right	dysplasia in right medial frontal gyrus	7	82±21
5	F	25	19	TLE	right amygdala	normal	2	96±34
6	F	28	23	TLE	mesio-temporo-polar right, mesio-temporal left	normal	19	65±20
7	M	33	24	TLE	independent bi-occipito-temporal left and right	bi-occipito-temporally abnormal gyral pattern	6	197±122
8	M	28	19	PLE	parietal left	dysplasia in left inferior parietal gyrus	7	121±41

F female, *M* male, *FLE* frontal lobe epilepsy, *PLE* parietal lobe epilepsy, *MRI* magnetic resonance imaging, *TLE* temporal lobe epilepsy

Table 2 Patient characteristics: Surgery type and outcome

ID	Surgery type	Outcome
1	resection mesio-temporo-polar right	aura- and seizure-free for more than 3 years
2	–	–
3	resection temporo-lateral left	aura- and seizure-free for more than two and a half years
4	lesionectomy	continuing seizures for half a year, since then seizure-free for more than one and a half years
5	resection temporo-polar right	single seizure 1 year after second surgery, currently seizure free
6	resection mesio-temporo-polar right	seizure-free for more than one and a half years, rare auras
7	–	–
8	–	–

brief, the temporal derivative (slope) of the iEEG signals was estimated by the differences

$$dX_i(t) = X_i(t+1) - X_i(t) \tag{1}$$

where i=1,…,M and t denotes temporal sampling points (t=*1,...,T-1*). The absolute value of the slope provides an appropriate characterization of epileptiform EEG since it is large for both slow, high amplitude signals as well as fast, low amplitude signals (Schindler et al. 2001). The absolute slopes were normalised by dividing by their standard deviation during a reference period of 120 s starting 5 min before visual seizure onset, and were smoothed by a lagging moving average with window length 5 s. For each iEEG channel the presence of epileptiform activity was defined by whether the normalised absolute slope exceeded the value 2.5 (Schindler et al. 2007b).

Bivariate Interrelation Measure: Slope Cross-Correlation

As the EEG slopes of Eq. (1) are good markers for epileptiform activity, and since seizures typically become manifest as pathological neuronal synchrony, the correlation patterns of these signals were also investigated. In the present paper we used a statistical and linear interrelation measure as opposed to dynamical nonlinear interrelation measures (Breakspear 2004). Specifically, the equal-time (zero-lag) cross-correlation was calculated from the slope of the signals according to the formula

$$C_{ij} = \frac{1}{L}\sum\nolimits_{t=1}^{L} p_{ij}(t) \tag{2}$$

where the sum runs over the products

$$p_{ij}(t) = \widetilde{dX_i}(t)\widetilde{dX_j}(t) = scc_{ij}(t) \tag{3}$$

and L=*T-1*. The tilde denotes signal normalization to zero mean and unit variance over the whole length of the selected data L. We termed the interrelation measure defined in Eq. (2) as *"slope cross-correlation"* (SCC). For later comparison we also state the definition of ordinary cross-correlation (CC) by Eq. (2) with L=T and

$$p_{ij}(t) = \widetilde{X_i}(t)\widetilde{X_j}(t) = cc_{ij}(t) \tag{4}$$

Multivariate Analysis: Measures Derived from the Eigenvalues and Eigenvectors of Correlation Matrices

To analyse multivariate EEG recordings the $M \times M$ matrix $\mathbf{C}$ of (slope or ordinary) correlation coefficients defined in Eqs. (2) and (3) or (4), was computed for analysis windows of length two seconds. Depending on the sampling rate, the windows contained either T=1,024 or T=2,048 sampling points and were shifted forward in time along the recordings in steps of 1 s. The correlation matrices $\mathbf{C} \in \{\mathbf{CC}, \mathbf{SCC}\}$

Table 3 Characteristics of the iEEG used for diagnostics

ID	Type of iEEG electrodes	No. of iEEG contacts	No. of artifact-free iEEG contacts
1	2 Fo, 4 strips	40	34
2	2 Fo, 4 strips	40	38
3	2 depth, 5 strips	56	56
4	2 depth, 10 strips	100	92
5	1 depth, 12 strips	102	99
6	3 depth, 9 strips	104	102
7	8 strips	62	59
8	1 depth, 1 grid	72	68

Fo foramen ovale, *iEEG* intracranial electroencephalogram

were diagonalised by solving the equation $\mathbf{C}\ \mathbf{v}_l=\lambda_l\ \mathbf{v}_l$, i.e. *eigenvalues* λ_l and *eigenvectors* $\mathbf{v}_l$ were calculated ($l=1,\ldots,M$). For a brief summary of mathematical properties of correlation matrices, eigenvalues and eigenvectors, the interested reader is referred to the Supplementary Material.

In the present study the total amount of EEG correlation in an analysis window was quantified using the spectrum of the M eigenvalues λ_l of the correlation matrices **CC** and **SCC**. The coefficient TCS of the *total correlation strength* (Müller et al. 2008)

$$TCS = \frac{1}{M-1}\sum_{l=1}^{M}|\lambda_1 - 1| \tag{5}$$

measures the normalised absolute deviations of the eigenvalues λ_l from the special case $\lambda_1 \equiv 1$, which is attained for matrices with ones on the diagonal and zeroes elsewhere (i.e. the correlation matrix representation of a hypothetically uncorrelated system). For the correlation matrices **CC** and **SCC,** the coefficient TCS ranges between 0 (for uncorrelated EEG channels in the limit $T\rightarrow\infty$) and 1 (for M identical EEG signals). Note that the network topology and not only the average correlation strength influences the value of TCS.

The *collectivity* of the eigenvectors $\mathbf{v}_l$ was quantified by their number of principal components (Plerou et al. 2002; Müller et al. 2005)

$$c_l = \frac{1}{M\sum_{i=1}^{M} v_{il}^4} \tag{6}$$

which measures the fraction of contributing channels. $c_l=1$ if all channels "*i*" contribute equally to $\mathbf{v}_l$. If, on the other hand, only a single channel contributes, $c_l=1/M$. Typically the eigenvector $\mathbf{v}_M$ corresponding to the largest eigenvalue λ_M (abbreviated as "largest eigenvector" henceforth) has very large collectivity (Plerou et al. 2002; Utsugi et al. 2004).

In addition, the *temporal stability* of the eigenvectors $\mathbf{v}_l$ was assessed by following the evolution of their scalar products with template vectors $\mathbf{V}_l$:

$$\sigma_l = \sum_{i=1}^{M} v_{il} V_{il} \tag{7}$$

The $\mathbf{V}_l$ were defined as the normalised mean of eigenvectors $\mathbf{v}_l$ of the matrices **CC** and **SCC** over a reference segment of length 120 s commencing 5 min before the visually determined seizure onset. A scalar product σ_l near 1 therefore implies an eigenvector (i.e. correlation pattern) close to that observed during the reference segment. Fluctuations in this value over time indicate instability in the eigenvector (i.e. temporal fluctuations in the correlation patterns).

Model Data

The performance of the interrelation measures **SCC** and **CC** is compared using a test system that is capable of exactly reproducing linear properties of real world EEG signals (power spectrum, auto-correlation, amplitude distribution) whilst also allowing for tunable cross-correlation between the signals (Rummel et al. 2008). In this model, surrogates (Schreiber and Schmitz 2000) of two channels of an interictal iEEG segment are taken as input and broadband correlation is introduced by mixing common and individual components. A coupling parameter k allows tuning between independent signals for $k=0$ and perfect (anti-)correlation for $k=\pm 1$.

Correlation measures should satisfy two important requirements. First, fluctuations should be small in order to provide reliable correlation estimates for a small number of trials (often a single trial). Second, correlation estimates should depend monotonically on the coupling strength; otherwise it remains unclear whether larger correlation estimates are indeed caused by larger inter-dependencies between signals. Here we assess both characteristics using the nonparametric ρ measure based on the U-statistic of the Mann–Whitney-Wilcoxon test (Herrnstein et al. 1976; Herrnstein 1979). $\rho \approx 0.5$ indicates a large overlap between two arbitrarily shaped distributions, whereas $\rho \approx 0$ and $\rho \approx 1$ indicate complete separation.

Statistical Evaluation

For simplicity of presentation we restricted our eigenvector analysis to properties of the largest eigenvector $\boldsymbol{v}_M$. Relative changes of the contribution of iEEG channels "*i*" at a given time step (as measured by the squared components v_{iM}^2), with respect to a pre-ictal reference interval were studied non-parametrically. To this end a 120 s EEG epoch starting 5 min before seizure onset (the same epoch as used for defining epileptiform activity and for defining the template vector) was used to sample the distribution of v_{iM}^2 under pre-ictal conditions. Components that deviated from this null distribution on the significance level $\alpha=0.01$ in the direction of larger ("local eigenvector excess") or smaller ("local eigenvector depletion") values were graphically displayed in red and blue, respectively.

The correlation of dynamical changes of collective activity on different spatial scales was examined by testing for correlations between the onset times of epileptiform activity and the onset times of local eigenvector excess or depletion. To this end, onset times s_i of epileptiform activity on channel "*i*" (as objectively defined by the slope criterion of sect. Univariate Analysis) as well as the time of first significant ictal excess x_i and the time of first significant ictal depletion d_i ,of v_{iM}^2 were determined. If channel "*i*" did not reveal epileptiform activity, excess, or depletion, s_i, x_i and d_i were set to the visually detected seizure termination time. Subsequently, s_i, x_i and d_i were rank ordered (with ties given average ranks) and Spearman's rank correlation coefficients r_{sx} and r_{sd} (Siegel 1956)

were calculated together with their significances p_{sx} and p_{sd}. Correlations were rated as significant for $p<0.01$ and as marginally significant (trends) for $p<0.05$.

Results

Slope Cross-Correlation and Cross-Correlation of Model Data

To elucidate the differences between analysis based on the matrices **CC** and **SCC** we represent in panels a, d and g of Fig. 1 pairs of normalised iEEG signals. Contacts located on the electrode TPL, which records directly from the SOZ located in temporo-polar structures of the left hemisphere of an epilepsy patient, show a prominent high frequency component. This component is much less apparent in channel FZTL1, which records from left fronto-centro-temporal structures distant from the SOZ. The products defined in Eqs. (3) and (4) are displayed in the second and third row of the figure. The mean values of these functions over the whole length, T or $T-1$, represent the matrix elements $\mathbf{CC}_{ij}$ and $\mathbf{SCC}_{ij}$, respectively. The product, $cc_{ij}(t)$, displayed in panel b is dominated by the transient (and possibly spurious) anti-correlation of the signals near $t=1.0$ s and $t=1.4$ s. In contrast, $scc_{ij}(t)$ focuses on the concomitance of (fast) local signal extrema, which partition the time series into pieces of ascending and descending signal values regardless of (slow) high amplitude deviations in the original signals. Panels d to f show a close-up of the region 1.2 s$<t<$1.3 s. Here, $cc_{ij}(t)$ has very small values and $scc_{ij}(t)$ oscillates around the x-axis. The reason for this is that the extrema of the iEEG channels TPL6 and FZTL1 are out of phase (see Fig. 1 panel d). This is different for the channels TPL6 and TPL7 (Fig. 1 panels g to i), where extrema appear concomitantly and therefore lead to strictly positive $scc_{ij}(t)$.

In Fig. 2, the performance of **SCC** and **CC** is explored using the mixing model of (Rummel et al. 2008). Panel a shows the dependence of **CC** (red) and **SCC** (blue) on the coupling strength, k, for time series of duration 2 s ($T=2{,}048$) and $N=50$ independent repetitions. The mean estimate of both measures is almost identical. However, the fluctuations of **CC** are considerably larger than those of **SCC**. In panels b to e the dependence of signal to noise ratio and monotonicity of the measures on coupling, k, and

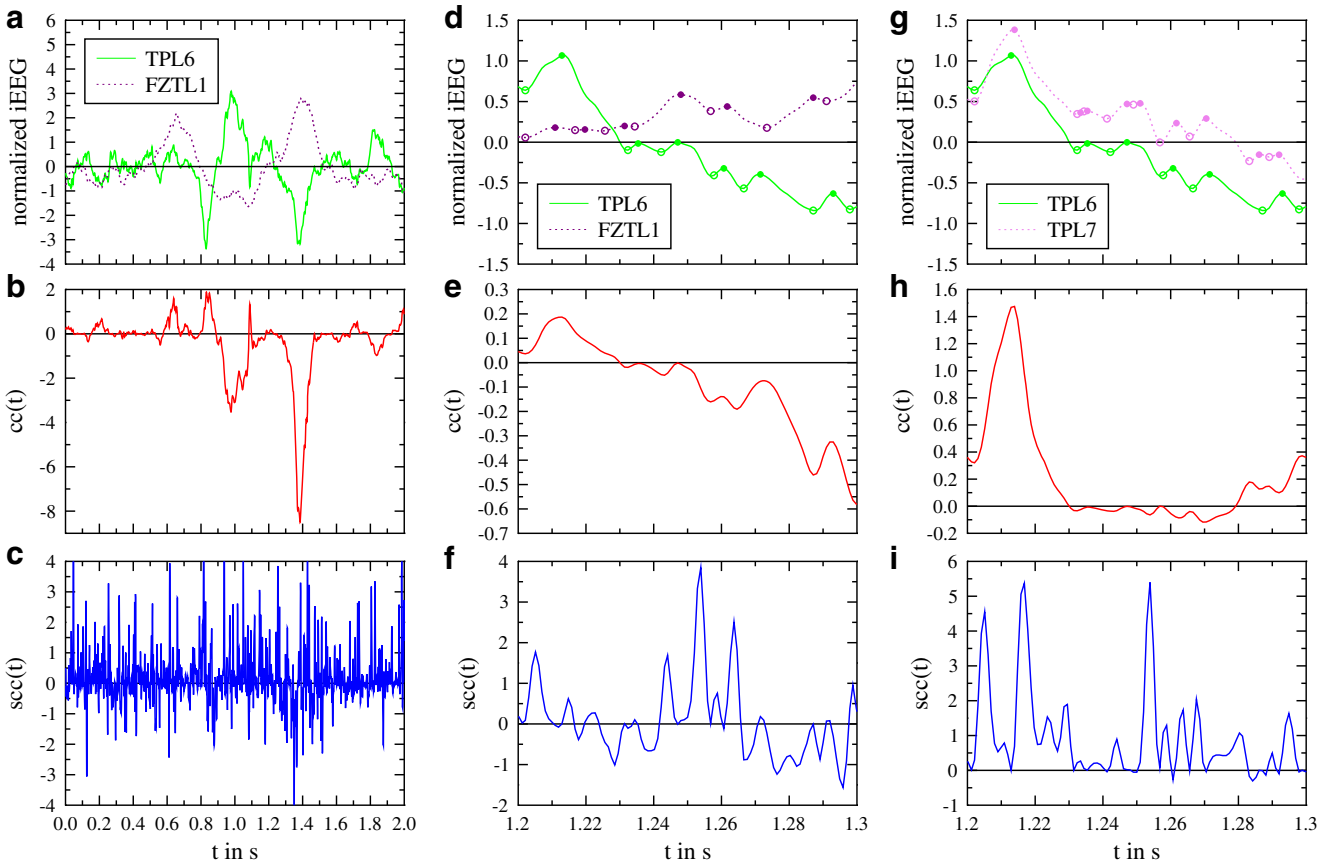

Fig. 1 (colour) Illustration of the performance of **CC** and **SCC** for selected iEEG signals. Panels **a**, **d** and **g** show normalized iEEG signals on different time scales. Local maxima are marked by full and local minima by open *dots* in panels **d** and **g**. In panels **b**, **c**, **e**, **f**, **h** and **i** comparison of the products p_{ij} defined in eqs. (3) and (4) is made

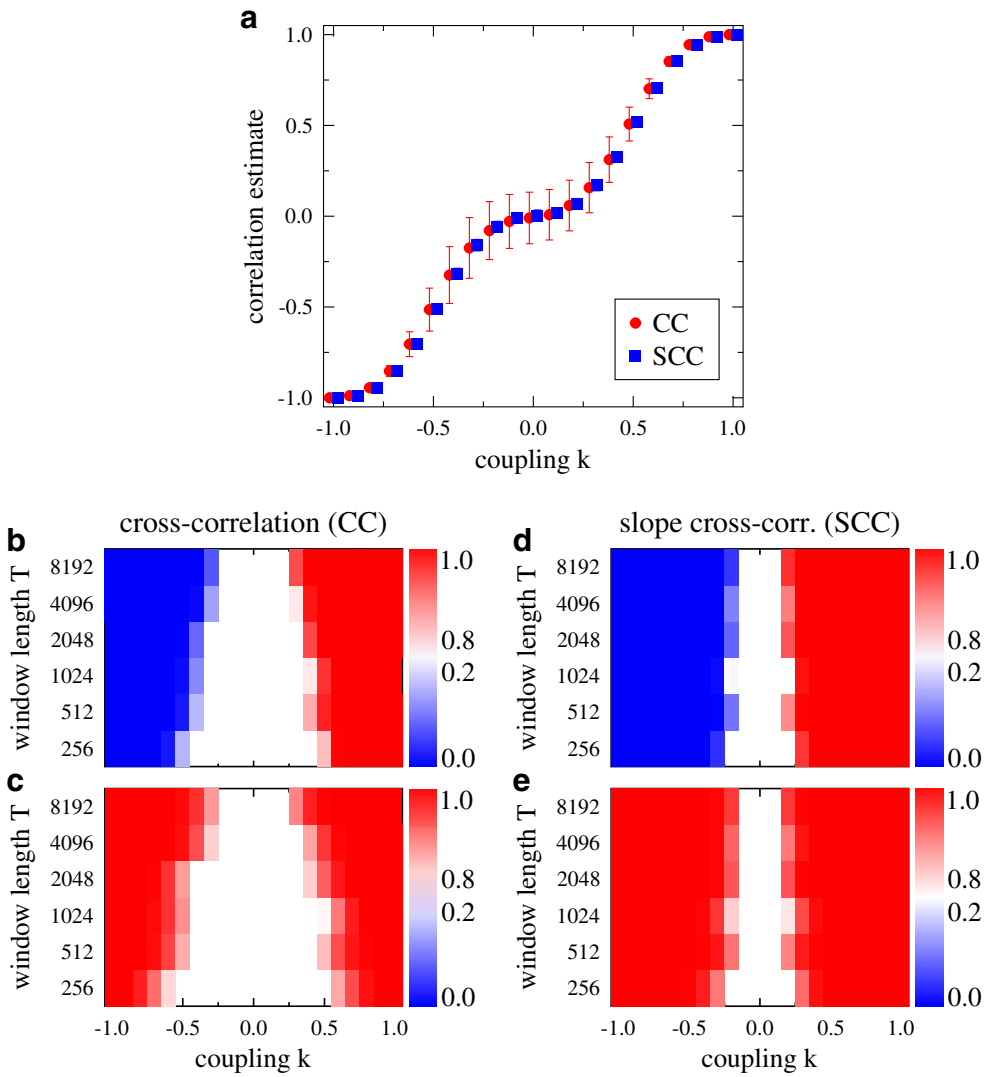

Fig. 2 (colour) Comparison of the performance of **CC** and **SCC** for model data. In panel **a** the correlation estimates are displayed for $T=2{,}048$ and $N=50$ independent repetitions. *Symbols* are slightly shifted along the x-axis to increase visibility. For **SCC** the *error bars* are often smaller than the symbol size. Panels **b** and **d** show the capability of distinguishing finite from zero coupling for **CC** and **SCC**, respectively. The capability of resolving the monotonicity of changes in coupling is displayed in panels **c** and **e** for **CC** and **SCC**, respectively

signal length, T, is investigated. Cases in which the distributions of correlation estimates are well separated appear in colour, whereas white regions indicate a large degree of overlap between distributions. In panels b and d, coloured areas indicate that a *finite* correlation estimate indeed corresponds to coupled signals (ρ for overlap of distributions of correlation estimates for coupled and uncoupled time series). Here, red ($\rho>0.8$) corresponds to positive correlation estimates whereas blue ($\rho<0.2$) indicates negative estimates. Similarly, coloured areas in panels c and e indicate *monotonicity*, i.e. the fact that a larger correlation estimate indeed corresponds to higher coupling (ρ for overlap of distributions of correlation estimates for time series coupled with k and $k\pm0.1$). Here red ($\rho>0.8$) corresponds to monotonic increase whereas blue ($\rho<0.2$) indicates monotonic decrease. The parameter scans show that **SCC** outperforms **CC** in two ways. First, the region in which for small $|k|$ finite correlation and monotonicity cannot be found is in general smaller (compare panels b and c for **CC** to panels d and e for **SCC**). Second, the T-dependence of performance is reduced for **SCC** (panels d and e), such that a similar precision can be obtained using analysis windows with shorter length, T.

iEEG of Epilepsy Patients

A representative example of the peri-ictal evolution of synchronisation at the smallest and intermediate spatial scale is given in Fig. 3 (seizure 2 of patient 3, visual seizure onset and termination as identified by an experienced epileptologist are marked by vertical lines). Panel a displays the epileptiform activity of iEEG channels. The first epileptiform activity (black) occurs in the iEEG channels 6 and 7, which record from left temporo-polar areas. Other temporo-polar (channel 2; note intermittent epileptiform activity of channels 2 and 4 at seizure onset), fronto-central (channels 18–20) and temporo-latero-basal (channels 12, 15 and 16) contacts are subsequently recruited into the ictogenic process. The surgical removal of the epileptogenic tissue (left temporo-polar strip electrode, iEEG channels 1–8 at the top

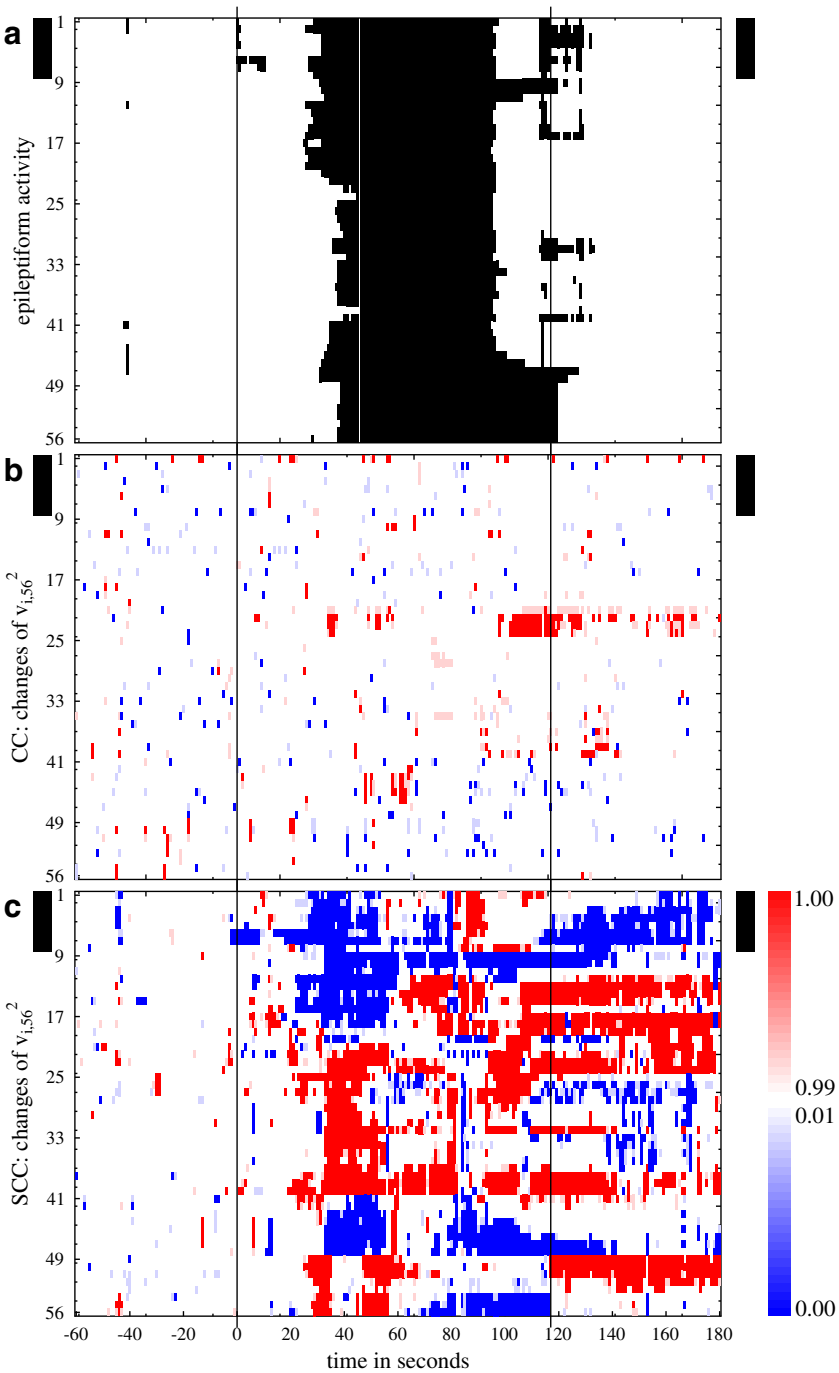

Fig. 3 (colour) Comparison of the temporal evolution of epileptiform activity (panel **a**, epileptiform: *black*, normal: *white*) with significant local eigenvector depletion (*blue*) and excess (*red*) as assessed by the largest eigenvector of the matrix **CC** (panel **b**) and the matrix **SCC** (panel **c**) for a peri-ictal segment containing focal onset seizure 2 of patient 3. Sequence of iEEG electrodes from top to bottom: left temporo-polar strip electrode (channels 1–8), left temporo-lateral-basal strip electrode (channels 9–16), left fronto-central-temporal strip electrode (channels 17–24), left fronto-orbital strip electrode (channels 25–32), left fronto-polar strip electrode (channels 33–40), left depth electrode (channels 41–48), right depth electrode (channels 49–56). Visually defined seizure onset and termination are marked by fully drawn *vertical lines*. The *bars* on the left and right margins mark the contacts recording from tissue whose surgical removal has led to seizure freedom for more than two and a half years (left temporo-polar structures)

of the panel, marked by bars on the left and right margins) led this patient to be seizure free for more than two and a half years.

Panels b and c show measures derived from eigenvectors of the **CC** and **SCC** matrix. Examples of the matrices, their eigenvalues and largest eigenvectors can be found in the Supplementary Material. Relative changes of the squared components v_{iM}^2 of the largest eigenvector of the (ordinary) cross-correlation matrix **CC** with respect to the reference segment are displayed in panel b. Increase is shown in red and decrease in blue. Aside from temporally unstable fluctuations, the largest eigenvector of the matrix, **CC,** calculated from the original iEEG signals, shows *no* significant local eigenvector depletion. Significant local eigenvector excess is observed in only a few fronto-central channels (22–24) and predominantly when close to seizure termination.

In contrast, a pronounced rearrangement of the pattern of the largest eigenvector of the slope cross-correlation matrix **SCC** occurs during the seizure (Fig. 3c). Its largest eigenvector undergoes significant and stable local depletion immediately at seizure onset and for exactly two of the four left temporo-polar iEEG contacts that first recorded epileptiform

activity (channels 6 and 7). As the seizure evolves, other channels with early epileptiform activity also deplete. Local excess of the squared eigenvector components v_{iM}^2 of the matrix **SCC** is predominantly found for fronto-orbital (channels 25–32) and fronto-polar contacts (channels 33–40), which are recruited late into the ictogenic process. In contrast to epileptiform activity, which disappears on most iEEG channels almost simultaneously after seizure termination (Fig. 3a), local depletion and excess of **SCC** eigenvector components with respect to the pre-ictal reference segment persist (Fig. 3c).

In Fig. 4 scalar measures derived from the eigenvalues and eigenvectors of the slope cross-correlation matrix **SCC** are displayed for the same seizure but on a different time scale. Panel a shows the evolution of the total correlation strength, TCS (defined in Eq. (5)). Correlation on the largest assessed spatial scale is remarkably stable before seizure onset and increases stepwise during the seizure. The seizure terminates when the total correlation nears its maximum value. After seizure termination, TCS slowly decays to the pre-ictal value. Panel b reveals an increased fluctuation in the evolution of collectivity (Eq. (6)) of the largest eigenvector of the matrix **SCC**. Collectivity is larger post-seizure than pre-seizure. The scalar product defined in Eq. (7) is very stable at values close to 1 before seizure onset, reflecting the high temporal stability of the largest eigenvector of the matrix **SCC** (panel c). During seizure, the scalar product deviates considerably from 1 and thus quantitatively summarises the ictal rearrangement of the largest eigenvector in a single value. The recovery of the scalar product to values near 1 indicates that the pre-ictal slope correlation pattern reappears approximately 2 min after seizure termination. Note, however, that in the post-ictal period, fluctuations are larger than those observed in the pre-ictal period. A compilation of the temporal evolution of TCS (Eq. (5)), collectivity (Eq. (6)), the scalar product (Eq. (7)) and localised excess and depletion of the largest eigenvector based on the matrices, **SCC** and **CC,** is given in the Supplementary Material for the first seizure of all patients studied.

Correlation between collective activity on the smallest and largest spatial scales was investigated on a single-seizure and single-patient basis by non-parametrically testing whether the onset times of epileptiform activity, s_i , are correlated with the onset times of significant local eigenvector depletion, d_i , or anti-correlated with the onset times of local eigenvector excess, x_i (see Methods). For **SCC** this analysis led to highly significant values of Spearman's rank correlation coefficients in both cases ($r_{sd}=0.810$, $p_{sd}<10^{-13}$ and $r_{sx}=-0.547$, $p_{sx}<10^{-4}$) in seizure 2 of patient 3. In contrast, local eigenvector depletion is not observed for **CC,** and correlation between onset times of epileptiform activity and local eigenvector excess is only marginally significant ($r_{sx}=-0.294$, $p_{sx}=0.028$). With the exception of two seizures during which anti-correlation between s_i and x_i is only marginally significant, the result for **SCC** is reproduced by all nine seizures of this patient (see Fig. 5d and e, patient 3). Also the spatial patterns of epileptiform activity and local **SCC** eigenvector depletion shown in Fig. 3a and c are reproducible for all seizures of this patient (data not shown).

A comprehensive representation of the results for all 60 seizures of all eight patients is given in Figs. 5 and 6. Panel a of both figures shows the significance of peri-ictal changes

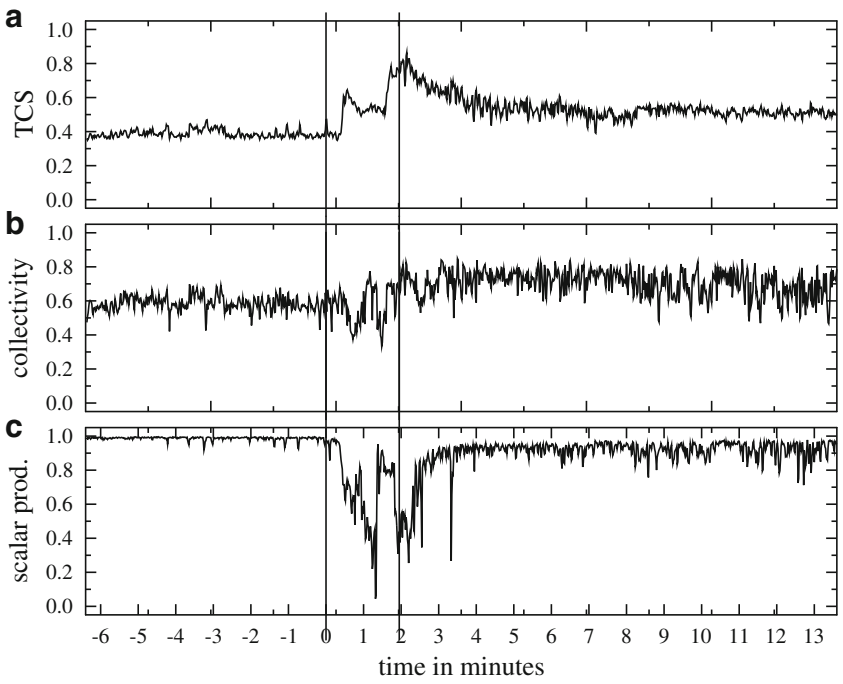

Fig. 4 Evolution of characteristics of the eigenvalue spectrum and the largest eigenvector of the matrix **SCC** for the same seizure as in Fig. 3 but on a different time scale. **a**) total correlation strength (TCS), **b**) collectivity of the largest eigenvector, **c**) scalar product of the largest eigenvector with the template. Visually defined seizure onset and termination are marked by fully drawn *vertical lines*

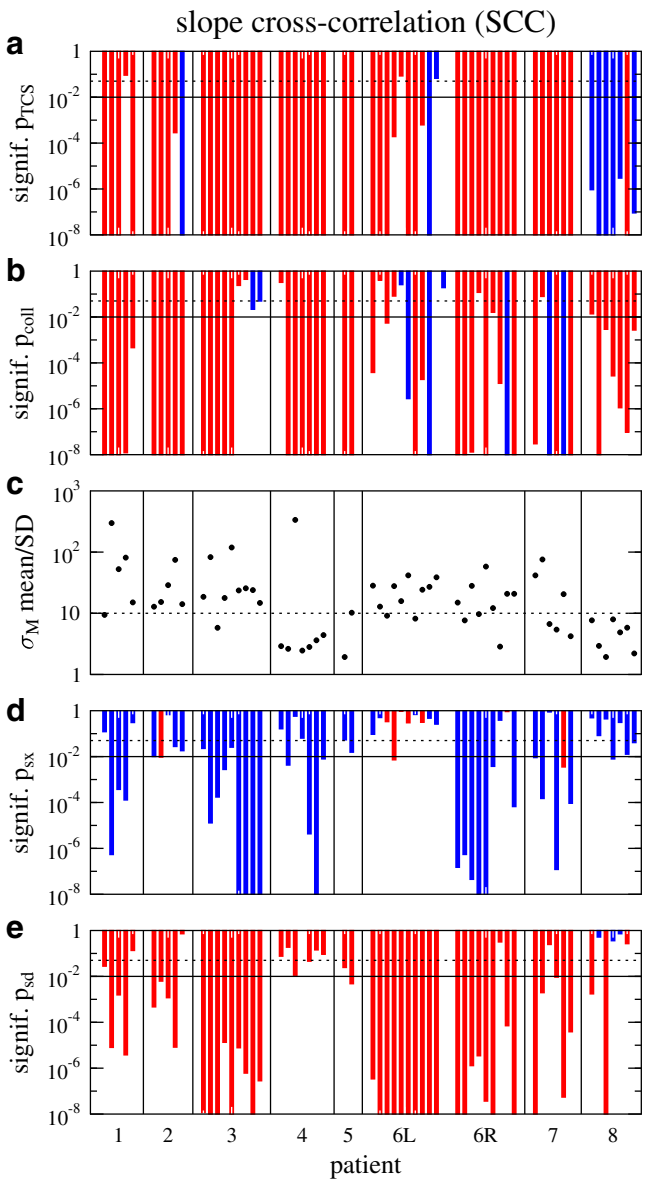

Fig. 5 (colour) Seizure-wise significances for tests based on properties of the matrix **SCC**. **a**) Significance for change of TCS between post-ictal and pre-ictal reference segment. **b**) Significance for change of collectivity of the largest eigenvector between post-ictal and pre-ictal reference segment. **c**) Ratio of mean and standard deviation of the scalar product σ_M within the pre-ictal reference segment. Significances p_{sx} (panel **d**) and p_{sd} (panel **e**) of correlation between onset times of epileptiform activity (s_i) and local **SCC** eigenvector excess (x_i) and depletion (d_i), respectively. *Longer bars* correspond to higher significance (smaller p). In the top panels *red* (*blue*) bars indicate TCS and collectivity increase (decrease). In the bottom panels bars are coloured in *red* (*blue*) if onset times are correlated (anti-correlated). As broken and fully drawn line the uncorrected significance levels $\alpha=0.05$ (marginally significant) and $\alpha=0.01$ (significant) are shown, respectively

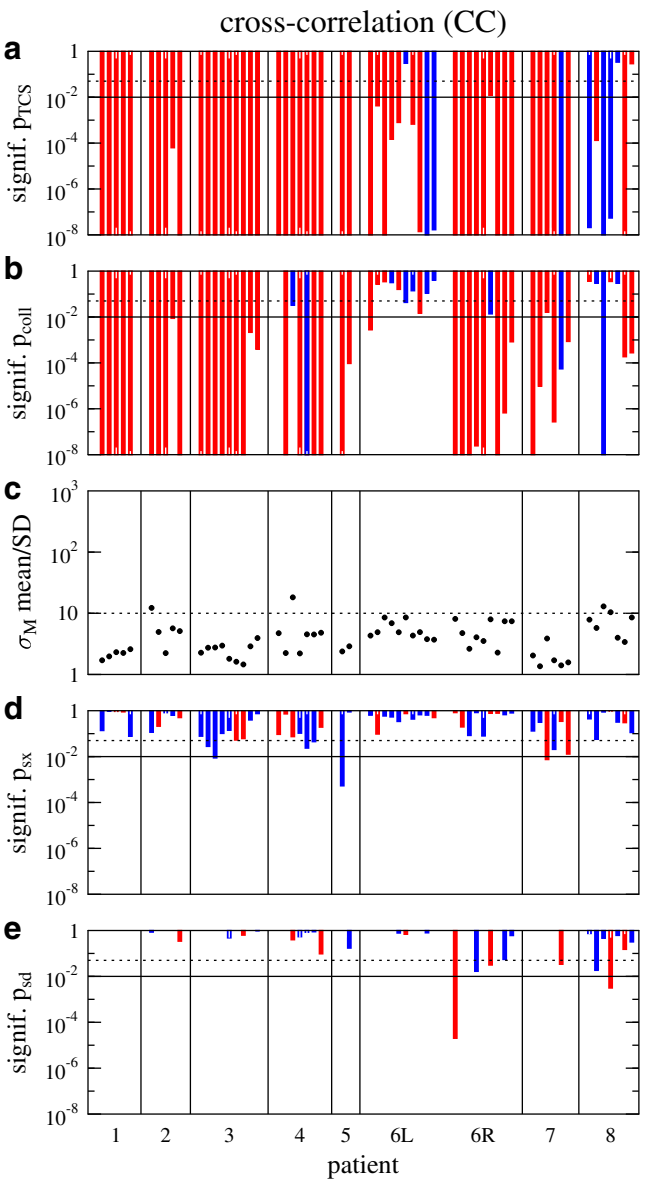

Fig. 6 (colour) Same as Fig. 5 but for the **CC** matrix

of correlation on the largest assessed spatial scale. For each seizure, TCS values (Eq. (5)) of a 120 s epoch immediately following seizure termination were compared to the pre-ictal reference segment. TCS increases significantly in 49 of 60 seizures (82 %) if calculated from **SCC** and in 50 seizures (83 %) if calculated from **CC**. Counter-examples are mainly confined to patient 8, for whom TCS predominantly decreases. The significance of changes in collectivity (Eq. (6)) of the largest eigenvectors is shown in panel b of Figs. 5 and 6. For **SCC** (**CC**), collectivity increases significantly in 42 (40) seizures (70 % / 67 %), does not change significantly in 13 (16) seizures (22 % / 27 %) and decreases significantly in only 5 (3) seizures (8 % / 5 %).

The stability of the scalar product (Eq. (7)) of the largest **SCC** and **CC** eigenvectors with the template vector is measured by the ratio of mean and standard deviation of this quantity over the reference segment, and displayed in panel c of Figs. 5 and 6. For **SCC** this quantity is larger than 10 in 45 of 60 seizures (75 %), reflecting a high stability of the

largest eigenvector. In contrast, for **CC** the ratio exceeds the value 10 in only 4 out of 60 seizures (7 %), indicating much larger variability.

Spatial rank correlations between the onset of epileptiform activity and the onset of local **SCC** eigenvector depletion are significant in more seizures than are anti-correlations with onset of local **SCC** eigenvector excess (at least marginally significant anti-correlation between s_i and x_i in 34 of 60 seizures (= 57 %, see Fig. 5d) vs. 46 of 60 seizures for correlation between s_i and d_i (= 77 %, see Fig. 5e)). The complete data is presented in Fig. 5 and patient-wise p-values are given in Table 4. Seizures in which neither anti-correlation nor correlation are significant are very rare for **SCC**. These situations predominantly occur in patients 4 and 8, whose recordings display considerably larger temporal fluctuations of the scalar product (Fig. 5c). Restricting the correlation analysis to patients for whom surgery was finally performed (patients 1, 3, 4, 5, 6), the significance of correlation remains unchanged in that 33 out of 42 cases display correlation between s_i and d_i (= 78 %) and 24 out of 42 cases display anti-correlation between s_i and x_i (= 57 %).

In contrast to **SCC**, spatial correlation between epileptiform activity and local eigenvector excess or depletion is almost never significant for the matrix **CC** (see Fig. 6d and e). The reason for this is that **CC** eigenvectors are much less stable over time than those derived from the matrix **SCC** (see Fig. 6c).

Summary and Discussion

In this study, we followed a systems-level approach combining univariate and multivariate analyses of the approximate first temporal derivatives ("slopes") of intracranial EEG signals. Specifically, we analysed the peri-ictal evolution of neuronal synchrony on three different spatial scales. Cooperative activity of a large number of neurons was assessed at the *smallest* scale accessible by iEEG (a single contact) and quantified in a univariate way by the absolute slopes of iEEG signals (Schindler et al. 2001). The ictal increase of the synchronous activity of thousands of neurons typically gives rise to high signal frequencies and/or large amplitudes (Penfield and Jasper 1954; Allen et al. 1992; Fisher et al. 1992; Alarcon et al. 1995; Schiff et al. 2000; Schindler et al. 2001; de Curtis and Gnatkovsky 2009).

Correlation on larger spatial scales was assessed by multivariate measures referred to as slope and ordinary cross-correlation matrices, **SCC** and **CC**, respectively. **SCC** contrasts with **CC** in that the former is not dominated by low frequency correlations, even though these frequencies have not been removed by filtering in a pre-selected pass band (Fig. 1). The reason for this is that correlations in the slope of the signal (measured by **SCC**) require periods in which the direction of the time series are the same, and is therefore related to the coincidence of positions of local extrema. Since extrema require a zero crossing of the derivative time series, they are tracked independently of the amplitude of activity at which they occur. Thus **SCC** provides a measure of co-evolution of time series in terms of the timing of events leading to changes in the direction of the signal. It is highest in periods where both their timing and the amplitude change between them is equivalent, and lowest in periods during which turning points in one time series are not replicated in the other. The temporal differentiation step in **SCC** implies spectral whitening and allows the examination of spatial patterns in higher frequencies, which play an important role during ictogenesis as well as for localisation of the SOZ (Schindler et al. 2001; Niederhauser et al. 2003; Worrell et al. 2004, 2008; Jacobs et al. 2009).

Our model results show that **SCC** provides interrelation estimates with a smaller degree of uncertainty than **CC** (Fig. 2). For the eigenvectors of matrices constructed from these measures this implies higher temporal stability (see comparison of Figs. 5c and 6c). Note that **SCC** shares similarities with the symbolic interrelation measures introduced in Liu (2004) and Wessel et al. (2009). However, the authors of these studies analysed a coarse grained description of the dynamics, taking into account only the direction of change. In contrast, the temporal derivative used in **SCC** also depends on the amount of change, making it more sensitive to large than to small changes.

Extending beyond previous studies (Schindler et al. 2007a, b), in which analyses were restricted to the dynamics of eigenvalues of correlation matrices, here the *intermediate* spatial scale was additionally assessed using the eigenvectors, $\boldsymbol{v}_M$, belonging to the largest eigenvalues, λ_M ,of the matrices **SCC** and **CC**. The collectivity of the largest eigenvector increases during most seizures (Figs. 4b, 5b and 6b). For **CC,** eigenvectors are not stable enough to reveal

Table 4 Patient-wise significances of Spearman correlation between localized onsets of epileptiform activity and eigenvector excess/depletion. "0" denotes zero to machine precision. In cases where significant deviation is not observed correlation analysis is not applicable ("n.a.")

ID	SCC		CC	
	p_{sx}	p_{sd}	p_{sx}	p_{sd}
1	$<10^{-10}$	$<10^{-12}$	0.31	n.a.
2	$<10^{-3}$	$<10^{-2}$	0.61	0.80
3	0	0	0.57	0.83
4	$<10^{-11}$	0.03	0.71	0.50
5	0.02	0.07	0.05	0.69
6	0	0	0.89	0.34
7	$<10^{-10}$	0	0.52	0.85
8	$<10^{-4}$	0.73	0.07	0.04

significant peri-ictal changes in the contribution of iEEG channels. However, the situation is different for **SCC** (Fig. 5c). When compared to the pre-ictal period, the relative contribution of the SOZ (i.e. those channels which are the first to show epileptiform activity) to the largest **SCC** eigenvector decreases during seizure. In contrast, the relative contribution of other brain areas increases (Fig. 3c; the interested reader is referred to the Supplementary Material, where an example of the first seizure is given for all patients). The observed local *"depletion"* and *"excess"* of the largest **SCC** eigenvector typically persisted into the post-ictal time period for several minutes. Note that this is in contrast to epileptiform activity, which ceased at seizure termination (Fig. 3a).

The mutual correlation between *all* the iEEG channels was quantified by the eigenvalue based total correlation strength (TCS) of the **SCC** and **CC** matrices (Müller et al. 2008). Similarly to the smallest spatial scale, on this *largest* spatial scale probed by iEEG, cooperative behavior increased ictally and seizures terminated when TCS neared its maximal value (Fig. 4a). With few exceptions, TCS calculated from **SCC** and **CC** was higher post-ictally than pre-ictally (Figs. 5a and 6a). Compared to small-scale synchrony, TCS decayed to the pre-ictal value more slowly after seizure termination. The increase of TCS corroborates earlier results by Schindler et al. (2007a, b), which were obtained using different quantifiers for the eigenvalue spectrum of the cross-correlation matrix **CC**. Our result is also consistent with recent graph theoretical findings revealing that iEEG networks are much denser in the late ictal and post-ictal period than before or during seizure (Kramer et al. 2010; Kramer and Cash 2012).

Our findings (higher TCS and eigenvector collectivity in the post-seizure phase; ictal decrease of the relative contribution of the SOZ and increase of more distant channels) indicate a stronger integration of the SOZ into collective brain dynamics after seizure than before seizure. This is consistent with the interpretation that during epileptic seizures, locally hypercorrelated and therefore functionally segregated brain areas are re-integrated into more collective brain dynamics. We propose that from a neurophysiological point of view, this dynamic reorganization of spatial correlation might be interpreted along the lines of a self-organised balancing or resetting mechanism. With regard to seizure treatment, this finding implies that pharmacological or physical methods that aim to increase the collectivity of electrical brain activity might be effective in terminating or even preventing epileptic seizures. Surprisingly, only sparse information is available regarding the effect of anti-seizure drugs on multi-scale EEG synchronization. Corresponding studies could reveal interesting extensions of pharmaco-EEG (Galderisi et al. 2006).

Of course, the idea that epileptic seizures might instantiate compensatory effects is long-standing, and was proposed as early as 1941 in the famous analogy of Lennox (1941), who likened epileptic seizures to the overflow of a water reservoir representing slowly accumulating ictogenic causes. The interpretation of seizures as resetting mechanisms has more recently been re-cast into the modern language of nonlinear dynamics (Iasemidis et al. 2004).

For the pre-ictal phase, our results are consistent with recent evidence regarding the relative isolation of seizure-generating brain areas. This was demonstrated by Warren et al. (2010) in terms of a relatively low degree of synchrony between local field potential recordings from seizure generating and non-seizure generating brain regions. That the pre-ictal brain state might be considered hypersegregated is also in line with the results of Mormann et al. (2003a, b), in which bivariate phase synchronization and cross-correlation measures were employed to detect significant desynchronization and decorrelation between pairs of selected iEEG channels. These changes often preceeded epileptic seizures by hours. The authors favoured the hypothesis that the reduced synchronization could be explained by the recording sites belonging to two different brain areas: one corresponding to neuronal tissue already involved in pathological synchronization progressing from the SOZ ("epileptic focus"), and one which maintains some form of physiologically synchronised process. Using a dynamical model of two interacting networks of integrate-and-fire neurons, these synchronization dynamics have recently been qualitatively reproduced by slowly increasing the mean depolarization of those neurons representing the SOZ (Feldt et al. 2007).

Correlation analysis between low-voltage rapid discharges (24–128 Hz) at selected sites has previously been undertaken by Wendling et al. (2003). The spatial reorganization of correlation suggested by our systems-level approach is consistent with these authors' finding of functional decoupling of distant brain sites at seizure onset. Our results are also in line with a very recent information theoretic approach of our group (Schindler et al. 2012). There, it was found that during seizure signal redundancy is locally increased in the SOZ, while mutual information with all other signals is decreased.

The findings of the present paper have potential implications for improving our understanding of the pathopyhsiology of epileptic seizures and for improving our ability to characterise epileptogenic tissue. These processes can be aided by studies of mechanistic models of nervous system tissue (Wendling et al. 2002; Breakspear et al. 2006; Lytton 2008; Goodfellow et al. 2011, 2012). The results of the present study, as well as future extensions along similar

lines, provide important new quantitative, spatio-temporal information that will support the modeling process.

In addition to general considerations regarding the pathophysiology of epileptic seizures, our results might also serve for a better characterization of the SOZ. Using **SCC** we observed a highly significant correlation of the sequence of onset of collective activity on different spatial scales in most seizures and patients (Fig. 5d,e). Seizures without spatial correlation between the onset of epileptiform activity and local **SCC** eigenvector depletion or excess were predominantly confined to patients 4 and 8, for whom the scalar product (Eq. (7)) with the template vector was less stable (see Fig. 5c). These were the only patients in our heterogeneous group to display features of dysplastic cortex on high resolution MRI (see Table 1). In the EEG the corresponding brain areas show permanent interictal spiking, which impairs the temporal stability of interrelation patterns as assessed by **SCC**. For the same reason, visual as well as more objective delineation of epileptiform from normal EEG activity is more difficult in these patients. In order to clarify the exact relation of altered spatial correlation between the onset times with the presence of cortical dysplasias subsequent studies are necessary using larger and more homogeneous patient groups.

The studied data set comprised five epilepsy patients who underwent resective surgery with a favorable outcome. For three patients, pre-surgical evaluation with iEEG and established clinical methods yielded results that prohibited surgery. We found that spatial correlation between onset times of epileptiform activity and local ictal depletion of **SCC** eigenvectors is independent from operability. Based on our findings, we propose that unless patients show MR visible cortical dysplasias, local ictal depletion of **SCC** eigenvectors could be used as an independent objective marker of the SOZ. We expect there to be situations in which local eigenvector depletion of the matrix **SCC** yields greater clarity regarding the location of the SOZ than the absolute slope criterion. Therefore **SCC** could provide important clinical information.

Information Sharing Statement

Patient data used for this publication contains confidential information and therefore cannot be shared. Essential analysis subroutines written in C can be obtained from the first author.

Acknowledgments C.R. and K.S. thank Markus Müller for fruitful discussions. This work was supported by Deutsche Forschungsgemeinschaft, Germany (grant RU 1401/2-1) and Schweizerischer Nationalfonds, Switzerland (projects 320030-122010 and 33CM30-124089). M.G. acknowledges financial support from the EPSRC and BBSRC (UK).

Conflicts of Interest None of the authors has any conflict of interest to disclose.

We confirm that we have read the Journal's position on issues involved in ethical publication and affirm that this report is consistent with those guidelines.

References

Alarcon, G., Binnie, C., Elwes, R., & Polkey, C. (1995). Power spectrum and intracranial EEG patterns at seizure onset in partial epilepsy. *Electroencephalography and Clinical Neurophysiology, 94*, 326–337.

Allen, P., Fish, D., & Smith, S. (1992). Very high-frequency rhythmic activity during SEEG suppression in frontal lobe epilepsy. *Electroencephalography and Clinical Neurophysiology, 82*, 155–159.

Bartolomei, F., Wendling, F., Bellanger, J. J., Reis, J., & Patrick, C. (2001). Neural networks involving the medial temporal structures in temporal lobe epilepsy. *Clinical Neurophysiology, 112*, 1746–1760.

Blumenfeld, H., McNally, K. A., Vanderhill, S. D., Paige, A. L., Chung, R., Davis, K., Norden, A. D., Stokking, R., Studholme, C., Novotny, E. J., Zubal, I. G., & Spencer, S. S. (2004). Positive and negative network correlations in temporal lobe epilepsy. *Cerebral Cortex, 14*, 892–902.

Blumenfeld, H., Varghese, G. I., Purcaro, M. J., Motelow, J. E., Enev, M., McNally, K. A., Levin, A. R., Hirsch, L. J., Tikofsky, R., Zubal, I. G., Paige, A. L., & Spencer, S. S. (2009). Cortical and subcortical networks in human secondarily generalized tonic–clonic seizures. *Brain, 132*, 999–1012.

Breakspear, M. (2004). "Dynamic" connectivity in neural systems. Theoretical and empirical considerations. *Neuroinformatics, 2*, 205–224.

Breakspear, M., Roberts, J. A., Terry, J. R., Rodrigues, S., & Robinson, P. A. (2006). A unifying explanation of generalized seizures via the bifurcation analysis of a dynamical brain model. *Cerebral Cortex, 16*, 1296–1313.

Bressler, S., & Kelso, J. (2001). Cortical coordination dynamics and cognition. *Trends in Cognitive Science, 5*, 26–36.

Dauwels, J., Eskandar, E., & Cash, S. (2009). Localization of seizure onset area from intracranial non-seizure EEG by exploiting locally enhanced synchrony. *Conference Proceedings IEEE Engineering in Medicine Biology and Society, 2009*, 2180–2183.

David, O., Blauwblomme, T., Job, A.-S., Chabardés, S., Hoffmann, D., Minotti, L., & Kahane, P. (2011). Imaging the seizure onset zone with stereo-electroencephalography. *Brain, 134*, 2898–2911.

de Boer, H. M., Mula, M., & Sander, J. W. (2008). The global burden and stigma of epilepsy. *Epilepsy & Behavior, 12*, 540–546.

de Curtis, M., & Gnatkovsky, V. (2009). Reevaluating the mechanisms of focal ictogenesis: the role of low-voltage fast activity. *Epilepsia, 50*, 2514–2525.

Elger, C. E., & Schmidt, D. (2008). Modern treatment of epilepsy: a practical approach. *Epilepsy & Behavior, 12*, 501–539.

Feldt, S., Osterhage, H., Mormann, F., Lehnertz, K., & Zochowski, M. (2007). Internetwork and intranetwork communications during bursting dynamics: Applications to seizure prediction. *Physical Review E, 76*, 021920.

Fisher, R., Webber, W., Lesser, R., Arroya, S., & Uematsu, S. (1992). High-frequency EEG activity at the start of seizures. *Journal of Clinical Neurophysiology, 9*, 441–448.

Frei, M. G., Zaveri, H. P., Arthurs, S., Bergey, G. K., Jouny, C. C., Lehnertz, K., Gotman, J., Osorio, I., Netoff, T. I., Freeman, W. J., Jefferys, J., Worrell, G., Le Van Quyen, M., Schiff, S. J., & Mormann, F. (2010). Controversies in epilepsy: Debates held

during the fourth international workshop on seizure prediction. *Epilepsy & Behavior, 19*, 4–16.

Friston, K. J., Tononi, G., Sporns, O., & Edelman, G. M. (1995). Characterizing the complexity of neuronal interactions. *Human Brain Mapping, 3*, 302–314.

Galderisi, S., & Sannita, W. G. (2006). Pharmaco-EEG: a history of progress and a missed opportunity. *Clinical EEG and Neuroscience, 37*, 61–65.

Goodfellow, M., Schindler, K., & Baier, G. (2011). Intermittent spike–wave dynamics in a heterogeneous, spatially extended neural mass model. *NeuroImage, 55*, 920–932.

Goodfellow, M., Schindler, K., & Baier, G. (2012). Self-organised transients in a neural mass model of epileptogenic tissue dynamics. *NeuroImage, 59*, 2644–2660.

Guye, M., Reis, J., Tamura, M., Wendling, F., Mc Gonigal, A., Patrick, C., & Bartolomei, F. (2006). The role of corticothalamic coupling in human temporal lobe epilepsy. *Brain, 129*, 1917–1928.

Herrnstein, R. J. (1979). Acquisition, generalization, and discrimination reversal of a natural concept. *Journal of Experimental Psychology: Animal Behavior Processes, 5*, 116–129.

Herrnstein, R. J., Loveland, D. H., & Cable, C. (1976). Natural concepts in pigeons. *Journal of Experimental Psychology: Animal Behavior Processes, 2*, 285–302.

Iasemidis, L. D., Shiau, D. S., Sackellares, J. C., Pardalos, P. M., & Prasad, A. (2004). Dynamical resetting of the human brain at epileptic seizures: Application of nonlinear dynamics and global optimization techniques. *IEEE Transactions on Biomedical Engineering, 51*, 493–506.

Jacobs, J., LeVan, P., Chatillon, C. E., Olivier, A., Dubeau, F., & Gotman, J. (2009). High frequency oscillations in intracranial eegs mark epileptogenicity rather than lesion type. *Brain, 132*, 1022–1037.

Kramer, M.A., Cash, S.S. (2012). Epilepsy as a disorder of cortical network organization, *Neuroscientist, 18*(4):360–372.

Kramer, M. A., Eden, U. T., Kolaczyk, E. D., Zepeda, R., Eskandar, E. N., & Cash, S. S. (2010). Coalescence and fragmentation of cortical networks during focal seizures. *Journal of Neuroscience, 30*, 10076–10085.

Lennox, W. (1941). *The causes of seizures. Science and seizures* (pp. 63–73). New York: Harper.

Lin, K., & Benbadis, S. R. (2009). Death and epilepsy. *Expert Review of Neurotherapeutics, 9*, 781–783.

Liu, Z. (2004). Measuring the degree of synchronization from time series data. *Europhysics Letters, 68*, 19–25.

Lüders, H. O. (2008). *Textbook of Epilepsy Surgery*. London: Informa Healthcare.

Lytton, W. (2008). Computer modelling of epilepsy. *Nature Reviews Neuroscience, 9*(8), 626–637.

McCormick, D. A., & Contreras, D. (2001). On the cellular and network bases of epileptic seizures. *Annual Review of Physiology, 63*, 815–846.

Majumdar, K. K., & Vardhan, P. (2011). Automatic seizure detection in ECoG by differential operator and windowed variance. *IEEE Transactions on Neural Systems and Rehabilitation Engineering, 19*, 356–365.

Mormann, F., Andrzejak, R. G., Kreuz, T., Rieke, C., David, P., Elger, C. E., & Lehnertz, K. (2003). Automated detection of a preseizure state based on a decrease in synchronization in intracranial electroencephalogram recordings from epilepsy patients. *Physical Review E, 67*, 021912.

Mormann, F., Kreuz, T., Andrzejak, R. G., David, P., Lehnertz, K., & Elger, C. E. (2003). Epileptic seizures are preceded by a decrease in synchronization. *Epilepsy Research, 53*, 173–185.

Müller, M., Baier, G., Galka, A., Stephani, U., & Muhle, H. (2005). Detection and characterization of changes of correlation structure in multivariate time series. *Physical Review E, 71*, 046116.

Müller, M., Baier, G., Rummel, C., & Schindler, K. (2008). Estimating the strength of genuine and random correlations in non-stationary multivariate time series. *Europhysics Letters, 84*, 10009.

Niederhauser, J. J., Esteller, R., Echauz, J., Vachtsevanos, G., & Litt, B. (2003). Detection of seizure precursors from depth-EEG using a sign periodogram transform. *IEEE Transactions on Biomedical Engineering, 50*, 449–458.

Penfield, W., & Jasper, H. (1954). *Hypersynchrony. Epilepsy and the functional anatomy of the human brain*. Boston: Little, Brown and Company.

Plerou, V., Gopikrishnan, P., Rosenow, B., Nunes Amaral, L. A., Guhr, T., & Stanley, H. E. (2002). Random matrix approach to cross correlations in financial data. *Physical Review E, 65*, 066126.

Rosenow, F., & Lüders, H. (2001). Presurgical evaluation of epilepsy. *Brain, 124*, 1683–1700.

Rummel, C., Müller, M., & Schindler, K. (2008). Data-driven estimates of the number of clusters in multivariate time series. *Physical Review E, 78*, 066703.

Schevon, C., Cappell, J., Emerson, R., Isler, J., Grieve, P., Goodman, R., Mckhann, G., Jr., Weiner, H., Doyle, W., Kuzniecky, R., Devinsky, O., & Gillam, F. (2007). Cortical abnormalities in epilepsy revealed by local eeg synchrony. *NeuroImage, 35*, 140–148.

Schiff, S., Colella, D., Jacyna, G. M., Hughes, E., Creekmore, J., Marshall, A., Bozek-Kuzmicki, M., Benke, G., Gaillard, W., Conry, J., & Weinstein, S. (2000). Brain chirps: spectrographic signatures of epileptic seizures. *Clinical Neurophysiology, 111*, 953–958.

Schiff, S. J., Sauer, T., Kumar, R., & Weinstein, S. L. (2005). Neuronal spatiotemporal pattern discrimination: The dynamical evolution of seizures. *NeuroImage, 28*, 1043–1055.

Schindler, K., Amor, F., Gast, H., Müller, M., Stibal, A., Mariani, L., & Rummel, C. (2010). Peri-ictal correlation dynamics of high frequency (80–200 Hz) intracranial EEG. *Epilepsy Research, 89*, 72–81.

Schindler, K., Elger, C. E., & Lehnertz, K. (2007). Increasing synchronization may promote seizure termination: Evidence from status epilepticus. *Clinical Neurophysiology, 118*, 1955–1968.

Schindler, K., Gast, H., Goodfellow, M., Rummel, C. (2012). On seeing the trees and the forest: Single-signal and multisignal analysis of peri-ictal intracranial EEG. *Epilepsia*. doi:10.1111/j.1528-1167.2012.03588.x.

Schindler, K., Leung, H., Elger, C. E., & Lehnertz, K. (2007). Assessing seizure dynamics by analysing the correlation structure of multichannel intracranial EEG. *Brain, 130*, 65–77.

Schindler, K., Wiest, R., Kollar, M., & Donati, F. (2001). Using simulated neuronal cell models for detection of epileptic seizures in foramen ovale and scalp EEG. *Clinical Neurophysiology, 112*, 1006–1017.

Schreiber, T., & Schmitz, A. (2000). Surrogate time series. *Physica D, 142*, 346–382.

Siegel, S. (1956). *Non-parametric Statistics for the Behavioral Sciences*. New York: McGraw-Hill.

Silberstein, R. B. (1995). Neuromodulation of neocortical dynamics. In P. L. Nunez (Ed.), *Neocortical dynamics and human EEG rhythms* (pp. 591–627). New York: Oxford University Press.

Smith, G., Ferguson, P. L., Saunders, L. L., Wagner, J. L., Wannamaker, B. B., & Selassie, A. W. (2009). Psychosocial factors associated with stigma in adults with epilepsy. *Epilepsy & Behavior, 16*, 484–490.

Spencer, S. S. (2002). Neural networks in human epilepsy: Evidence of and implications for treatment. *Epilepsia, 43*, 219–227.

Stam, C.J., Reijneveld, J.C. (2007). Graph theoretical analysis of complex networks in the brain. *Nonlinear Biomedical Physics, 1*(1), 3.

Takigawa, M., Fukuzako, H., Ueyama, K., Takeuchi, K., Fukuzako, T., & Nomaguchi, M. (1994). Developing of EEG print and its

preliminary technical application. *Japan Journal of Psychiatry Neurology, 48*, 91–97.

Tononi, G., Sporns, O., & Edelman, G. M. (1994). A measure for brain complexity: Relating functional segregation and integration in the nervous system. *Proceedings of the National Academy of Sciences, 91*, 5033–5037.

Uhlhaas, P. J., & Singer, W. (2006). Neural synchrony in brain disorders: Relevance for cognitive dysfunctions and pathophysiology. *Neuron, 52*, 155–168.

Utsugi, A., Ino, K., & Oshikawa, M. (2004). Random matrix theory analysis of cross correlations in financial markets. *Physical Review E, 70*, 026110.

Varela, F., Lachaux, J. P., Rodriguez, E., & Martinerie, J. (2001). The brainweb: Synchronization and large-scale integration. *Nature Review Neuroscience, 2*, 229–239.

Warren, C. P., Hu, S., Stead, M., Brinkmann, B. H., Bower, M. R., & Worrell, G. A. (2010). Synchrony in Normal and Focal Epileptic Brain: The Seizure Onset Zone is Functionally Disconnected. *Journal of Neurophysiology, 104*, 3530–3539.

Weder, B. J., Schindler, K., Loher, T. J., Wiest, R., Wissmeyer, M., Ritter, P., Lovblad, K., Donati, F., & Missimer, J. (2006). Brain areas involved in medial temporal lobe seizures: a principal component analysis of ictal spect data. *Human Brain Mapping, 27*, 520–534.

Wendling, F., Bartolomei, F., Bellanger, J., Bourien, J., & Chauvel, P. (2003). Epileptic fast intracerebral activity for spatial decorrelation at seizure onset. *Brain, 126*, 1449–1459.

Wendling, F., Bartolomei, F., Bellanger, J., & Chauvel, P. (2002). Epileptic fast activity can be explained by a model of impaired GABAergic dendritic inhibition. *European Journal of Neuroscience, 15*, 1499–1508.

Wessel, N., Suhrbier, A., Riedl, M., Marwan, N., Malberg, H., Bretthauer, G., Penzel, T., & Kurths, J. (2009). Detection of time-delayed interactions in biosignals using symbolic coupling traces. *Europhysics Letters, 87*, 10004.

Worrell, G. A., Gardner, A. B., Stead, S. M., Hu, S., Goerss, S., Cascino, G. J., Meyer, F. B., Marsh, R., & Litt, B. (2008). High-frequency oscillations in human temporal lobe: simultaneous microwire and clinical macroelectrode recordings. *Brain, 131*, 928–937.

Worrell, G. A., Parish, L., Cranstoun, S. D., Jonas, R., Baltuch, G., & Litt, B. (2004). High-frequency oscillations and seizure generation in neocortical epilepsy. *Brain, 127*, 1496–1506.

Zachry, W. M., III, Doan, Q. D., Smith, B. J., Clewell, J. D., & Griffith, J. M. (2009). Direct medical costs for patients seeking emergency care for losses of epilepsy control in a U.S. managed care setting. *Epilepsy & Behavior, 16*, 268–273.